Harvesting energy from CO_2 emissions

H.V.M. Hamelers[1], O. Schaetzle[1] , J.M. Paz-García[1] , P.M. Biesheuvel[1,2] and C.J.N. Buisman[1,2]*

[1] Wetsus, centre of excellence for sustainable water technology, Agora 1, 8934 CJ Leeuwarden, The Netherlands.

[2] Department of Environmental Technology, Wageningen University, Bornse Weilanden 9, 6708 WG Wageningen, The Netherlands.

KEYWORDS: CO2 utilization, capacitive electrodes, salinity gradient energy, monoethanolamine.

Abstract

When two fluids of different composition are mixed, mixing energy is released. This holds true for both liquids and gases, though in case of gas, no technology is yet available to harvest this energy source. Mixing the CO_2 in combustion gases with air represents a source of energy with a total annual worldwide capacity of 1570 TWh. To harvest the mixing energy from CO_2 containing gas emissions, we use pairs of porous electrodes, one selective for anions and the other selective to cations. We demonstrate that, when an aqueous electrolyte, flushed with either CO_2 or air, alternately flow between these selective porous electrodes, electrical energy is gained. The efficiency of this process reached 24% for deionized water as aqueous electrolyte

and 32% for 0.25 M monoethanolamine (MEA) solution as electrolyte. The highest average power density obtained with a MEA-solution as electrolyte was 4.5 mW/m^2, significantly higher than for water as electrolyte where the power density is 0.28 mW/m^2.

1. Introduction

Mixing two solutions of different composition leads to a mixture with a lower Gibbs energy content compared to the original two solutions (1). This decrease in the Gibbs function indicates the presence of mixing energy that can be harvested when a suitable technology is available.

Up until now, the use of the mixing process as a source of energy has only been exploited for mixing of aqueous solutions with a different salinity (2, 3). Mixing freshwater from rivers with seawater typically has an available work of ~3 kJ per L of freshwater (4). Several technologies are being developed to exploit this source of energy using semipermeable membranes (5), ion-selective membranes (2), double-layer expansion (6, 7) and ion-selective porous electrodes (8-13). The latter technology is based on the use of capacitive electrode cell pairs; similar to those used in supercapacitors (14,15) or in capacitive deionization (CDI) for water desalination (16-18). Another approach uses dry air at the cathode side to sustain a concentration cell; however such a cell works at the expense of water (19).

We investigate the possibility to harvest energy from CO_2 emissions. Wherever hydrocarbon fuels or biomass are combusted, i.e. converted to CO_2 and water, emissions containing high CO_2 concentrations (5%-20%) (20) compared to air (0.039%) are produced. This means that mixing combustion gas with air is an unexplored source of energy. To harvest this energy source we propose to contact both the CO_2 emission and air with an aqueous electrolyte. In aqueous solutions, CO_2 reacts with water to produce carbonic acid that itself dissociates into protons (H^+) and bicarbonate (HCO_3^-), which can further dissociate at high pH to carbonate ions (CO_3^{2-}). An

increase of the CO_2 pressure in the gas leads to an increase of the concentration of the ions in the aqueous solution. The resulting difference in the ion concentration between the air-flushed solution and the CO_2-flushed solution can be used to gain electrical energy. Here we show that it is possible to gain energy from mixing CO_2 emissions and air, opening up an additional source of energy.

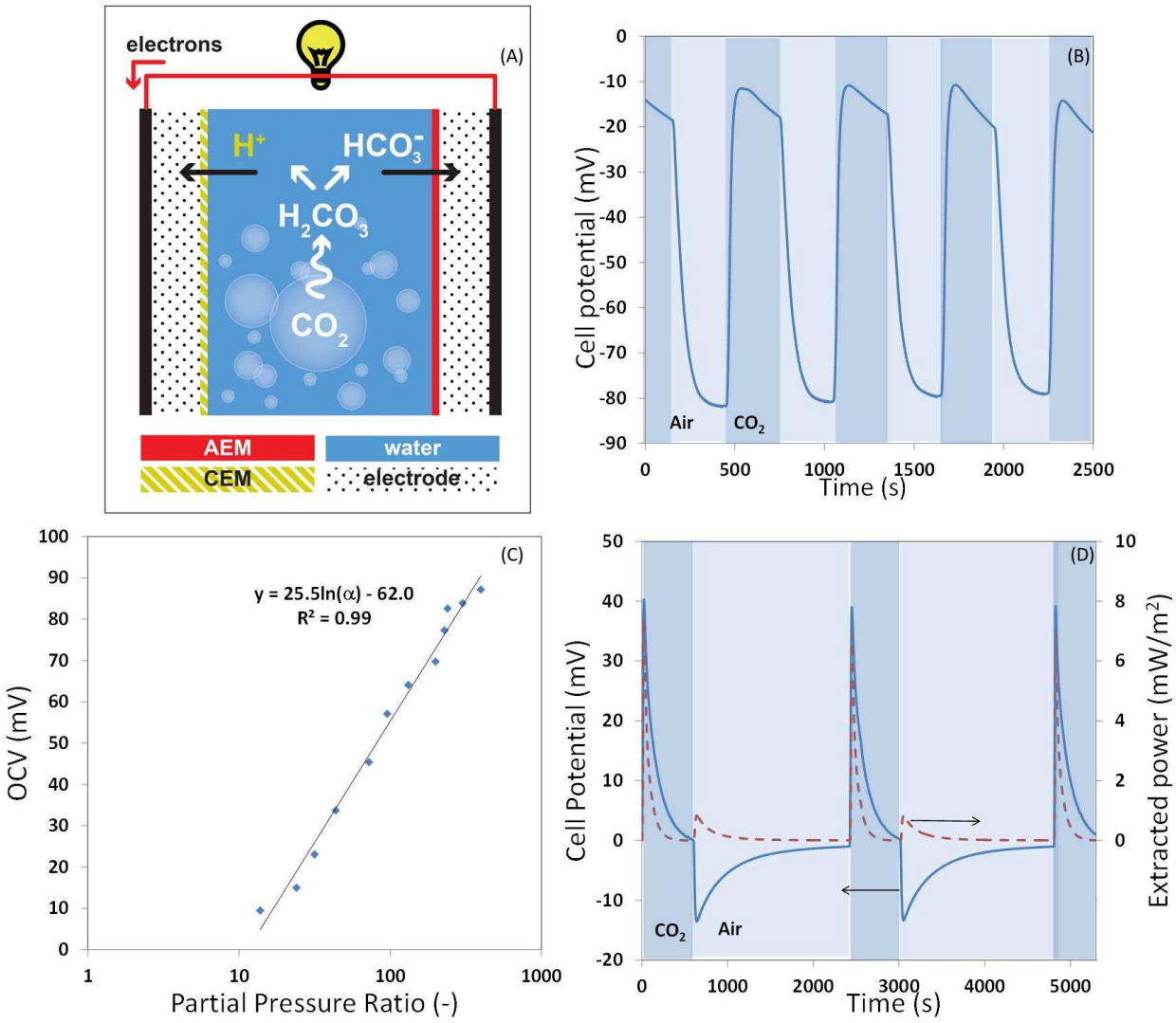

Figure 1. Harvesting of energy from CO_2 emissions in capacitive electrochemical cells. (**A**) Principle of the method: dissolved CO_2 dissociates in protons and bicarbonate ions, which diffuse into different electrodes due to the ion-selectivity of the membranes placed in front. The resulting membrane potential leads to the spontaneous generation of current. (**B**) Measured open circuit voltage (OCV) of the capacitive electrochemical cell alternatingly exposed to air-flushed water and CO_2-flushed water ($t_{air} / t_{CO_2} = 5 / 5\,\mathrm{min}$). The light blue area denotes the period during which air-flushed water is used, while the dark blue area denotes the period during which CO_2-

flushed water is used. (**C**) Relation between partial pressure ratio α and the measured OCV (**D**) Cycles of energy extraction at $R_{ext} = 22\,\Omega$ using water as electrolyte. The blue line shows the measured cell potential, the red dashed line shows the extracted power. The area colour code is the same as in panel B.

2. Materials and Methods

2.1 Research Setup

Our setup consisted of two tanks containing the electrolyte, i.e. deionized water or 0.25 M monoethanolamine (MEA) solution (reagent grade $\geq 99\%$, Sigma-Aldrich). One tank was flushed with air while the other was flushed with CO_2 gas (Air Products, 100% pure). Each tank is connected to the capacitive cell via a peristaltic pump (Cole-Parer, Masterflex L/S). The outlet of both pumps is connected to the inlet of the capacitive cell via a T shaped connector. Between each pump and the T connector, valves are placed to prevent backflow. Just before the inlet of the capacitive cell a small glass vessel was installed containing a pH probe. The glass vessel was filled with 5 mm diameter glass beads in order to minimize the dead volume in this vessel. The pH probe was connected to an online pH data logger (RSG 30, Endress+Hauser). Cell potential under open circuit conditions, or in a closed circuit via an external load, was measured with a multimeter (Fluke 8846A 6-1/2 Digit precision Multimeter) with the anion exchanging electrodes connected to the ground of the multimeter. Fig. S1 in the SI shows a drawing of the setup and a picture of the actual setup.

2.2 Capacitive cell

The capacitive cell consists of two capacitive electrodes, one covered by a cation-exchange membrane (CEM) and the other covered by an anion exchange membrane (AEM). The cell used

in all experiments (see electronic supporting information) consists of a flat flow-through cell built by stacking together a number of layers: 1) an aluminium plate used as endplate, 2) a hollowed polymethylmethacrylate plate (PMMA) with a graphite plate socket used as current collector, 3) a silicon gasket for sealing the cell and to create space for the capacitive electrode, 4) a capacitive porous electrode made of a graphite foil current collector coated with an activated carbon layer, 5) a CEM to create selectivity to cations (protons), 6) a Teflon gasket to create room for the spacer, 7) a polymeric spacer to allow the flow between the membranes and 7) an anion-exchange membrane to create selectivity to anions (bicarbonate ions). The rest of the cell consists of a parallel layout of gasket, capacitive electrode, PMMA plate and aluminum end-plate.

2.3 Materials

The porous carbon electrodes are prepared by mixing activated carbon powder with a binder solution. They are produced by the following method: carbon powder (DLC Super 30, Norit, Amersfoort, the Netherlands, BET area = 1600 m^2g^{-1}) is dried in an oven at 105 ^oC for 24 hours. Then, the carbon powder is mixed with a solution of polyvinilidene fluoride (PVDF; KYNAR HSV 900, Arkema Inc. Philadelphia, USA) in 1-methyl 2-pyrrolidone (NMP; Merck Schuchardt OHG, Hohenbrunn, Germany), in a ball mill grinder (PM 100, Retsch, Haan, Germany) for 30 min at 450 rpm. The resulting slurry is cast on a graphite foil (Coidan graphite product LTD, 500 µm thick), using a 500 µm casting knife to produce a carbon film. The film is immersed in deionized water to remove the remaining NMP. The final product is a solidified carbon film of 270 µm thickness, containing 10 w% PVDF binder. The electrode dimensions were 25 cm × 2 cm and the total mass of activated carbon used in the cell is 2.0 g. As a pre-treatment, the electrodes are soaked in CO_2-flushed deionized water or in MEA solutions.

Anion-exchange membrane (AEM, Fumasep FAS, Fumatech, Germany, 30-40 μm thickness), and cation exchange membrane (CEM, Fumasep FKS, Fumatech, Germany, 30-40 μm) are pre-treated by soaking them during 24 h in a 0.25 M HCl solution for the CEM and in a 0.25 M $KHCO_3$ solution for the AEM. During this period, the soaking solutions were refreshed 2 times. A polymer spacer is used to create a flow channel (PA 6.6 fabric, Nitex 03-300/51, Sefar, Heiden, Switzerland, thickness = 200 μm).

2.4 Operation of the system

Flushing of the solutions with gas takes place in a separate vessel, allowing equilibrium to be established between the gas and the water prior to entering the cell (SI,Fig. S1). Two solutions are used: water flushed with pure gaseous CO_2, and water flushed with air. The solutions are pumped through a spacer channel between the two ion exchange membranes. In all experiments, the flow of the CO_2-flushed water through the device is alternated with the flow of air-flushed water. These two steps together constitute one cycle. The water is free from other salts, the temperature is 20°C and the setup operates at atmospheric pressure.

2.5 Open circuit voltage (OCV) measurements

The maximum OCV values are obtained by measuring the maximum cell potential difference when changing from the air-flushed solution to the CO_2-flushed solution under no current conditions (SI,Fig. S3).

2.6 Operation of the cell for determining the effect of the CO_2 content on OCV

For the measurement of the effect of the CO_2 content on the OCV, the system is operated in the following modified way: At first, two tanks, 1 and 2, are respectively flushed with air and CO_2. We start cycling (i.e alternatively pumping the CO_2-flushed solution and the air-flushed solution every 5 min) and record the cell potential and the pH. After at least three cycles showing a stable

maximum OCV, we stop flushing CO_2 into tank 2 and start flushing air instead (just as in tank 1). As a result, the CO_2 content of this solution in tank 2 will slowly decrease. From the measured pH value of the effluent of the tanks, we calculate the partial pressure ratio $\alpha = p_{CO_2,high} / p_{CO_2,low}$ as $\alpha = 10^{2(pH_L - pH_H)}$ where pH_L is the pH of the low p_{CO_2} solution and pH_H the pH of the high p_{CO_2} solution (see SI section 2. and Fig. S4).

2.7 Calculation of the energy extracted, the average power and efficiency

The extracted energy is calculated using the following relation: $W = \int I.Edt$ where $W(\mathrm{J})$ is the extracted work, $E(\mathrm{V})$ the cell potential and $I(A)$ is the current, while the integration takes place over the duration of the cycle (s). Efficiencies reported in this study were obtained by dividing the measured extracted energy in one cycle by the theoretically available energy in an optimal cycle $W_{max} = V_{cell,max} * Q$, where $W_{max}(J)$ is the maximum extracted work possible in the cycle, $V_{cell,max}(V)$ the theoretical maximum OCV (in this study, the maximum potential is 206 mV) and $Q(C)$ the amount of charge exchanged in one cycle.

2 Results and discussion

In the first experiment (Fig. 1B) we operate the cell under open circuit conditions and alternately supply the air-flushed solution and the CO_2-flushed solution each for 5 minutes. The open circuit voltage (OCV) showed a stable cyclic response, clearly following the solution alterations, indicating the CO_2 pressure as the driving force. There is a clear asymmetry in the time response with a faster change from air to CO_2 (about 60 seconds when water is used as the electrolyte) compared to the change from CO_2 to air (around 180 seconds when water is used as the electrolyte). There is drift in the OCV for the CO_2-flushed solution, a drift that we explain in

terms of the effect of carbonic acid that diffuses through the ion exchange membranes, driven by the high concentration in the CO_2 flushed solution. The cell voltage is determined by four separate potentials, the membrane potential of the two membranes and the double layer potential of the two porous carbon electrodes (11). Inside and after passage of the membrane the carbonic acid dissociates partly into protons and bicarbonate resulting in higher ion concentrations in the pore water of the electrodes. This ion concentration increase will lower the membrane potential as the concentration difference over the membrane decreases. The ions can also be specifically adsorbed to the porous electrode, changing in this way the surface charge and thus the double layer potential (9). In case of changing NaCl concentrations such a fast drift is not observed (11), this is also not expected as NaCl fully dissociates. In an ideal approximation, the theoretical upper limit for the cell potential is given by the equation, $V_{\text{cell, max}} = RTF^{-1}\ln(\alpha)$, in which $\alpha = p_{CO_2,\text{high}} / p_{CO_2,\text{low}}$ is the partial pressure ratio (see SI section 1). For our experimental conditions, we expect $V_{\text{cell, max}} = 206$ mV at $p_{CO_2,\text{high}} = 1$ bar and $p_{CO_2,\text{low}} = 390$ ppm. To further show that the partial pressure ratio is the driving force of the voltage response, we measure the OCV for different partial pressure ratios. We use in this experiment air-flushed water and CO_2-flushed water of different CO_2 saturation levels. Fig. 1C shows the relationship between the OCV and partial pressure ratio applied. As expected from equation 1, the OCV in Fig. 1C increases linearly with the natural logarithm of the partial pressure ratio. The slope of this curve equals 25.5 mV, which coincides well with the theoretical expected value of $RTF^{-1} = 25.4$ mV. The measured difference in membrane potential at $p_{CO_2} = 1$ bar is around 90 mV, 44% of the theoretically expected value of 206 mV. As the slope is in accordance with the theory, we believe that the lower OCV is caused by an increase of the CO_2 content of the air-saturated flow. As the concentration in the air-flushed water is in the order of 1 μM, any release of physically

adsorbed CO_2 (in the cell or tubing for example) will easily increase the concentration and, in this way, lower the partial pressure ratio and consequently the OCV. This analysis is consistent with the observed asymmetry of the OCV (fig. 1B), namely that it takes longer to go from a high concentration to a low concentration than vice versa. We further explored this idea by pumping the air saturated water through the system for 900 minutes and we measured the OCV to be 136 mV.

It is possible to produce electricity by connecting the two electrodes through an external load $R_{ext}(\Omega)$ (Fig. 1D), allowing electrons to flow between the electrodes. When exposed to the CO_2-flushed water, the membrane potential will drive electrons from the anion specific electrode to the cation specific electrode. This transport of electronic charge leads to an excess charge in each electrode. To maintain electroneutrality, this excess charge is compensated by counterion adsorption at the electrode surface (Fig. 1A), until equilibrium is reached between the membrane potential and the double layer potential and the cell voltage becomes zero. When the CO_2-flushed solution is replaced by the air-flushed one, the new membrane potential will reverse these processes and drives the ions out of the electrodes, back into the flowing solution, until the system reaches its new equilibrium where again the cell potential is zero. This clear zero cell potential is typical for an energy-producing mode of operation of the cell. However, under open circuit condition there is no charge transport and there is thus no possibility for the electrode double layer potential to equilibrate with the membrane potential. As a consequence, the potential will only change as the result of the change in membrane potential, but it is not self-evident that a zero cell potential will be reached because the electrode potentials remain constant.

Cycles can be repeated by alternatingly pumping the two solutions. The obtained electrical power is equal to $P = V^2 / R_{ext}$. The power production was measured for several external

resistance values to find the one at which the highest average power density was achieved. For an external load of 22 Ω, stable cycles are obtained with a peak and average power density of 6.2 mWm^{-2} and an average power density of 0.28 mWm^{-2} is obtained (Fig. 2B). The energy efficiency of this cycle is 12.4% and during each cycle 6.4 m*J* was extracted (SI, Fig. S5).

It is possible to further improve the power density by increasing the absorption of CO_2 in the solution. For this, a new series of experiment is done using as electrolyte a 0.25 M solution of monoethanolamine (MEA) instead of deionized water. MEA is a moderately strong base, with alkaline buffer properties that is conventionally used to absorb CO_2 from exhaust gases (21, 22). The OCV for the MEA electrolyte was measured in a similar way as in case of water as electrolyte. The OCV did not differ appreciably, and in both cases was around 90 mV. The same drift is again observed for the CO_2-saturated solution, which is in line with the explanation of carbonic acid diffusion (SI, Fig. S6).

The higher CO_2 absorption leads to an increase of the concentration of the dissociated ions, reflected in an increase of the conductivity (13.6 mS/cm for the MEA solution and 0.04 mS/cm for the solution without MEA). The increase in the ionic concentration leads to cycles where the voltage across the load is higher and the system responds more quickly compared to the use of deionized water (30 mJ extracted in 720 s compared to 6 mJ extracted in 2240 s respectively) (Fig. 2A). The initial cell potential measured after a change of electrolyte solution has an upper limit determined by the OCV However when using a load, part of the OCV is lost due to the internal resistance of the cell, yielding a lower cell potential. Because the OCV is similar whether water or MEA was used as electrolyte, and because the use of the MEA solution gives a lower internal resistance, the resulting initial cell potential will be higher when using MEA as electrolyte. Operation at 5 Ω results in the best performance in terms of energy extracted. For

this condition, the peak power density equals 31.7 mWm^{-2} and an average power density of 4.5 mWm^{-2} is obtained. The energetic efficiency using this load was 20.1% and the energy extracted per cycle was 32 mJ (SI, Fig.S5). The highest P_{avg} is, in case of the use of MEA, a factor 16 higher compared to the use of deionized water (Fig. 2B).

The highest energetic efficiency is found at the highest resistance: 24% in the case of using water as electrolyte, and 32% in case of the 0.25 M MEA solution (Fig. 2B). With higher external resistances, the current will be smaller and, consequently, the energy losses due to the internal resistance will also be smaller. In all cases the use of a MEA solution gives a higher power density at the same energetic efficiency.

After use, the he MEA solution can be easily recycled by transferring it back to the sparging vessels. In these vessels air flushing will remove the transferred CO_2, while, in the CO_2-flushed vessel, new CO_2 will be absorbed.

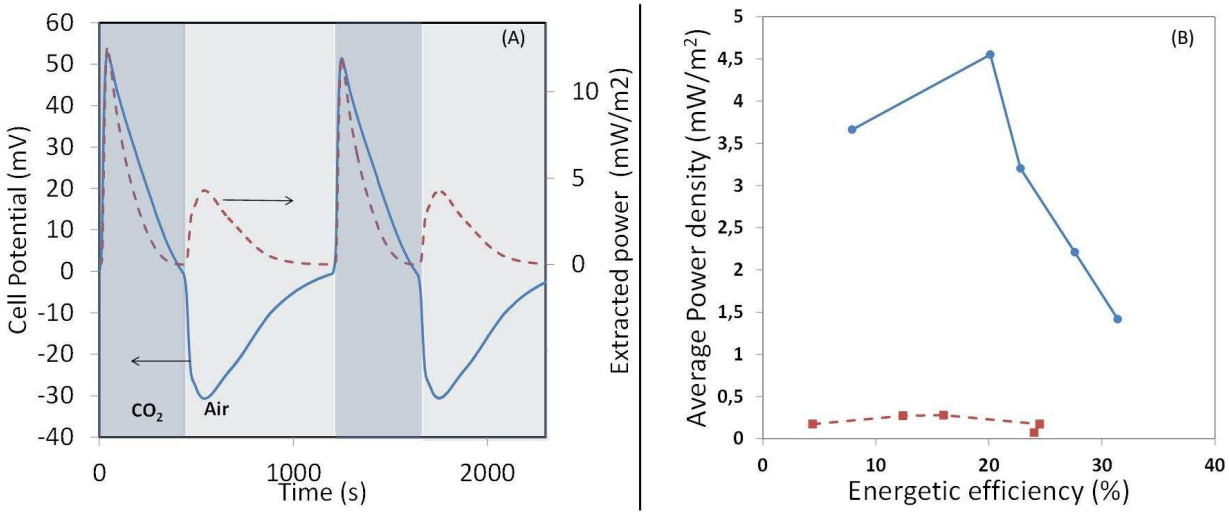

Figure 2. Effect of the using an aqueous solution of monoethanolamine (MEA). (**A**) Example cycle for energy harvesting at $R_{ext} = 22\,\Omega$ with MEA 0.25 M. The blue line shows the measured cell potential, and the red dashed line shows the extracted power. The area colour code is the

same as in Fig. 1 B (**B**) Average power densities for different external loads as function of the energetic efficiency. Data obtained for water (red dashed line) and the MEA solution 0.25 M (blue line) are shown.

The worldwide annual CO_2 production in power plants running on hydrocarbon sources is ~12 GT (12×10^{12} kg, 2010) (23, 24), from which ~9 GT are coming from coal fired power plants and ~2 GT from gas and oil fired power plants. A coal-fired power plant produces an exhaust gas with typically 12.7 % CO_2, while the CO_2 content in exhaust gas from a gas-fired power plant is lower, usually around 7.5% CO_2 (25). The amount of available energy depends on the composition of the gases and the temperature at which the mixing process takes place. For gas-fired and coal-fired power plants, mixing the exhaust gas at a temperature of 20 °C gives, respectively, 236 kJ and 265 kJ per kg of CO_2, equivalent to 28 kJ and 50 kJ per kg of exhaust gas emitted (see SI section 2 and S7). This means that worldwide around 850 TWh of additional electricity is available yearly in the flue gases of power plants without additional CO_2 emissions.

The technology might also be suited for other stationary sources like industry and residential heating. These other stationary sources emit together around 11 GT of CO_2 (23, 24) yearly. Although the CO_2 content might be different, using the lower value for gas combustion we can estimate another potential of ~720 TWh yearly. Together, these CO_2 emissions have a potential of about 1570 TWh yearly, equivalent to 400 times the Hoover Dam (USA), without adding to global CO_2 emissions.

Both the air flushed and CO_2 flushed solutions were prepared by gas sparging, as this is a simple technology easily applied in the laboratory. However, sparging is an energy intensive operation that has been extensively studied in wastewater treatment. There, the specific aeration efficiency is in the range 0.6-7.5 kg O_2/kWh depending on the technology applied. (26) Even

using the most efficient aeration technology we estimate we need 350 kJ per mol CO_2. This calculation shows that the use of sparging to contact the gases with the electrolyte consumes more energy than is produced. Therefore to make our technology applicable more efficient mass transfer equipment must be selected and investigated, such as membranes, which include a passive mass transfer layer. The possible role of the carbonic acid in the OCV drift should be explored as this lowers the OCV and thus lowers energy extraction. Considering the size of the energy source (about 1570 TWh) and the much high energy density of CO_2 emissions compared to mixing seawater and freshwater makes CO_2 emissions an interesting energy source to explore further. Here we have shown that using ion-selective porous electrodes we can indeed harvest this source of energy. However, other technologies used for harvesting salinity gradient energy such as RED or PRO (3) can be also considered.

Corresponding Author
*bert.hamelers@wetsus.nl

Author Contributions

The manuscript was written through contributions of all authors. All authors have given approval to the final version of the manuscript.

ACKNOWLEDGMENT

This work was performed in the TTIW-cooperation framework of Wetsus, centre of excellence for sustainable water technology (www.wetsus.nl). Wetsus is funded by the Dutch Ministry of Economic Affairs, the European Union Regional Development Fund, the Province of Fryslân, the City of Leeuwarden and the EZ/Kompas program of the "Samenwerkingsverband Noord-Nederland". Part of this work was performed for the Capmix project funded by the European Union Seventh Framework Programme (FP7/2007-2013) under grant agreement n° 256868.

ASSOCIATED CONTENT

Supporting Information.

The supporting information includes:

- Theory on the open circuit cell potential, Relationship between partial pressure ratio and pH difference and Theory on the maximal mixing energy.

- 5 figures

This material is available free of charge via the Internet at http://pubs.acs.org/journal/estlcu

ABBREVIATIONS

CDI, capacitive deionization; MEA monoethanolamine; CEM, cation exchange membrane; AEM, anion exchange membrane; OCV, open circuit voltage.

REFERENCES

1. Denbigh, K. G. *The Principles of Chemical Equilibrium*; Cambridge University Press: 1957
2. Pattle, R. E. Production of Electric Power by mixing Fresh and Salt Water in the Hydroelectric Pile. *Nature* **1954**, 174, (4431), 660-660.
3. Logan, B. E.; Elimelech, M. Membrane-based processes for sustainable power generation using water. *Nature* **2012**, 488, (7411), 313-319.
4. Post, J. W.; Veerman, J.; Hamelers, H. V. M.; Euverink, G. J. W.; Metz, S. J.; Nymeijer, K.; Buisman, C. J. N. Salinity-gradient power: Evaluation of pressure-retarded osmosis and reverse electrodialysis. *Journal of Membrane Science* **2007**, 288, (1-2), 218-230.
5. Loeb, S.; Norman, R. S. Osmotic Power Plants. *Science* **1975**, 189, (4203), 654-655.
6. Brogioli, D. Extracting Renewable Energy from a Salinity Difference Using a Capacitor. *Physical Review Letters* **2009**, 103, (5), 058501-4.
7. Brogioli, D.; Zhao, R.; Biesheuvel, P. M., A prototype cell for extracting energy from a water salinity difference by means of double layer expansion in nanoporous carbon electrodes. *Energy & Environmental Science* **2011**, 4, (3), 772-777.
8. La Mantia, F.; Pasta, M.; Deshazer, H. D.; Logan, B. E.; Cui, Y. Batteries for Efficient Energy Extraction from a Water Salinity Difference. *Nano Letters* **2011**, 11 (4) 1810-1813
9. Brogioli, D.; Ziano, R.; Rica, R. A.; Salerno, D.; Kozynchenko, O.; Hamelers, H. V. M.; Mantegazza, F. Exploiting the spontaneous potential of the electrodes used in the capacitive mixing technique for the extraction of energy from salinity difference. *Energy & Environmental Science* **2012**, 5, (12), 9870-9880.
10. Sales, B. B.; Saakes, M.; Post, J. W.; Buisman, C. J. N.; Biesheuvel, P. M.; Hamelers, H. V. M. Direct Power Production from a Water Salinity Difference in a Membrane-Modified Supercapacitor Flow Cell. *Environmental Science & Technology* **2010**, 44, (14), 5661-5665.
11. Liu, F.; Schaetzle, O.; Sales, B. B.; Saakes, M.; Buisman, C. J. N.; Hamelers, H. V. M., Effect of additional charging and current density on the performance of Capacitive energy extraction based on Donnan Potential. Energy & Environmental Science **2012**, 5, (9), 8642-8650.
12. Boon, N.; van Roij, R. 'Blue energy' from ion adsorption and electrode charging in sea and river water. *Molecular Physics* **2011**, 109, (7-10), 1229-1241.
13. Rica, R. A.; Ziano, R.; Salerno, D.; Mantegazza, F.; Bazant, M. Z.; Brogioli, D. Electro-diffusion of ions in porous electrodes for capacitive extraction of renewable energy from salinity differences. *Electrochimica Acta* **2013**, 92, 304-314.
14. Merlet, C.; Rotenberg, B.; Madden, P. A.; Taberna, P.-L.; Simon, P.; Gogotsi, Y.; Salanne, M. On the molecular origin of supercapacitance in nanoporous carbon electrodes. *Nature Materials* **2012**, 11, (4), 306-310.

15. Kondrat, S.; Perez, C. R.; Presser, V.; Gogotsi, Y.; Kornyshev, A. A. Effect of pore size and its dispersity on the energy storage in nanoporous supercapacitors. *Energy & Environmental Science* **2012**, 5, (4), 6474-6479.
16. Porada, S.; Weinstein, L.; Dash, R.; van der Wal, A.; Bryjak, M.; Gogotsi, Y.; Biesheuvel, P. M., Water Desalination Using Capacitive Deionization with Microporous Carbon Electrodes. *ACS Applied Materials & Interfaces* **2012**, 4, (3), 1194-1199.
17. Porada, S.; Zhao, R.; van der Wal, A.; Presser, V.; Biesheuvel, P. M. Review on the science and technology of water desalination by capacitive deionization. *Progress in Materials Science*, **2013**, http://dx.doi.org/10.1016/j.pmatsci.2013.03.005.
18. Zhao, R.; Biesheuvel, P. M.; van der Wal, A. Energy consumption and constant current operation in membrane capacitive deionization. *Energy & Environmental Science* **2012**, 5, (11), 9520-9527.
19. Dreizler, A. M.;Roduner, E. A fuel cell that runs on water and air. *Energy & Environmental Science* **2010**, 3, (6),761-764.
20. Wall, T. F. Combustion processes for carbon capture. *Proceedings of the Combustion Institute* **2007**, 31, (1), 31-47.
21. Mergler, Y.; Gurp, R. R.-v.; Brasser, P.; Koning, M. d.; Goetheer, E. Solvents for CO2 capture. Structure-activity relationships combined with vapour-liquid-equilibrium measurements. *Energy Procedia* **2011**, 4, 259-266.
22. Rochelle, G. T. Amine Scrubbing for CO2 Capture. *Science* **2009**, 325, (5948), 1652-1654.
23. IEA Key World Statistics 2012; International Energy Agency: 2012.
24. Statistics, I. CO2 Emissions from Fuel Combustion - Highlights; International Energy Agency: 2012.
25. Xu, X.; Song, C.; Wincek, R.; Andresen, J. M.; Miller, B. G.; Scaroni, A. W., Separation of CO2 from Power Plant Flue Gas Using a Novel CO2 “Molecular Basket” Adsorbent. *Fuel chemistry* **2003**, 48, (1), 2.
26. Shiau, C.; Oxygen transfer in bubble and bubbleless aeration systems, PhD thesis, Department of Civil and Mining Engineering, University of Wollongong, 1995.